Project Title:

Blood Flow simulation with cell movement.

Name:
○Shigeho NODA, Xiaobo Gong
Laboratory at RIKEN:
Head Office for Information Systems and Cybersecurity
The R&D Group
Computational Engineering Applications Unit

1. Background and purpose of the project, relationship of the project with other projects

In human microcirculation, the red blood cell(RBC) occupies the most volume fraction of blood and it is the main factor which influences the blood rheological properties [1]. Some pathological process is closely related to the motion and deformation of the RBC in a microchannel such as the oxygen transport and the filtration of the RBC in spleen [2]. The motion of RBCs in a microchannel with different geometry is generally studied [3].

Some diseases can influence the mechanical properties of the RBC such as sepsis, malaria, type 2 diabetes mellitus, hereditary spherocyte and so on, which can reduce the deformation ability of the RBC. For example, Park [4] studied the membrane stiffness of RBCs parasitized by Plasmodium falciparum. It is found the they are 4~20 times stiffer than normal RBCs. Recognizing the mechanical properties of the RBC can assist the disease diagnosis. Many technologies are developed to measure the mechanical properties. For example, micropipette aspiration, optical tweezers and observation done by atomic force microscope. But these methods are difficult to operate and consume a lot of time thus cannot deal with a large amount of blood sample in a short period. It is of great significance to design a high-throughput method to measure the mechanical properties of the RBC.

The core of related works is evaluating the relationship between motion or deformation index and the mechanical properties of the RBC in different flow condition and then propose a scheme to characterize the mechanical properties of RBCs quickly. Many researches focus on the motion of RBC in a channel with a square cross section. In such channel, the fluid field exhibits asymmetry which results the asymmetry of the deformation of the RBC. This will introduce difficulty in measuring of the deformation index of the RBC. A tube with a circular cross section can alleviate the asymmetry. Moreover, the motion of a single RBC in a narrow tube (diameter~4μm) is never been studied and the motion and deformation index may be more sensitive to the change of mechanical properties of the RBC which is better for the characterization. So we study the steady motion of a single RBC in a circular-section narrow tube. Different steady shapes are presented as function of the membrane elastic shear modulus. And we explain the relationship between the cell velocity and the membrane shear modulus using lubrication theory qualitatively. The extra pressure drop which shows the flow resistance introduced by cell is discussed with regard to different elastic shear modulus.

2. Specific usage status of the system and calculation method

In FY2019, about 2,700,000 core*hours were used for my Quick Use project. We used a parallel program based on OpenMp and MPI to numerically simulate the motion and deformation of red blood cell in confined micro-tube.

In the present work, the immersed boundary method is used to simulate the interaction between cell membrane and flow field. According to the Continuum Mechanics [5], the deformation gradient tensor $\mathbf{F}$ is defined as $\mathbf{F} = \partial \mathbf{x} / \partial \mathbf{X}$, in which $\mathbf{X}$

represents the coordinate of a point under a stretch-free condition and $\mathbf{x}$ represents its current coordinate. In reality, the thickness of the RBC membrane, which is only about 2nm, three orders smaller than the diameter of RBCs, can be neglected. Then the membrane is modeled as two dimensional and the surface deformation tensor is defined as:

$$\mathbf{F}_s = \mathbf{P} \cdot \mathbf{F} \cdot \mathbf{P}_R \qquad (1)$$

$\mathbf{P} = \mathbf{I} - \mathbf{nn}$ and $\mathbf{P}_R = \mathbf{I} - \mathbf{n}_R\mathbf{n}_R$ are surface projection tensors. $\mathbf{n}$ and $\mathbf{n}_R$ are the unit normal vectors in the current coordinate and reference stress-free coordinate, respectively. Then define the surface left Cauchy-Green deformation tensor as

$$\mathbf{B}_s = \mathbf{F}_s \cdot \mathbf{F}_s^{\mathrm{T}}. \qquad (2)$$

Its invariant is defined as

$$I_1 = \mathrm{tr}(\mathbf{B}_s) - 2$$
$$I_2 = \left(\mathrm{tr}(\mathbf{B}_s)^2 - \mathrm{tr}(\mathbf{B}_s^2)\right)/2 - 1 \qquad (3)$$

Rewrite them as:

$$c_1 = I_1 + 1 \quad \text{and} \quad c_2 = I_2 + 1 \qquad (4)$$

The strain energy function derived by Skalak et al. [5] is used in the paper:

$$W_s = \frac{E_s}{8}(c_1^2 + \alpha c_2^2 - 2(\alpha+1)c_2 + \alpha + 1) \qquad (5)$$

E_s is an elastic shear modulus and $\alpha(\alpha \gg 1)$ is an index to resist the surface dilation. Then the in plane stress is given by

$$\boldsymbol{\tau} = \frac{2}{\sqrt{c_2}}\left(\frac{\partial W_s}{\partial c_1}\mathbf{B}_s + c_2\frac{\partial W_s}{\partial c_2}\mathbf{P}\right) \qquad (6)$$

According to Pozrikidis [6], the transvers shear vector $\mathbf{q}$ is given by

$$\mathbf{q} = \left((\mathbf{P} \cdot \nabla) \cdot \mathbf{m}\right) \cdot \mathbf{P} \qquad (7)$$

$\mathbf{m}$ represents the bending moment which is modeled by a linear constative as following:

$$\mathbf{m} = E_b(\boldsymbol{\kappa} - \kappa_R\mathbf{P}) \qquad (8)$$

E_b is a bending stiffness. $\boldsymbol{\kappa}$ and κ_R represent the current Cartesian curvature and the reference mean curvature, respectively.

$$\boldsymbol{\kappa} = -\mathbf{P} \cdot \nabla\mathbf{n} \qquad (9)$$

$$\kappa_R = -\frac{1}{2}\mathrm{tr}(\mathbf{P}_R \cdot \nabla\mathbf{n}_R) = -\frac{1}{2}\mathrm{tr}(\nabla\mathbf{n}_R) \qquad (10)$$

We define the membrane as Γ, the domain surrounded by Γ is Ω_1, and the outer domain as Ω_2. Using $[*]$ to represent the jump of a variable at the membrane, the following conditions can be derived:

$$[\mathbf{v}] = 0, [\mathbf{n} \cdot \boldsymbol{\sigma}] = \mathbf{f}_\Gamma \qquad (11)$$

$\mathbf{v}$ is the velocity vector, $\boldsymbol{\sigma}$ is the stress tensor of fluid, $\mathbf{n}$ is the unit normal vector of Γ pointing outside Ω_1 and $\mathbf{f}_\Gamma$ is the surface singular force vector.

Considering the force balance of a infinitely small membrane patch, $\mathbf{f}_\Gamma$ can be given by:

$$\mathbf{f}_\Gamma = -\mathrm{Trace}[(\mathbf{P} \cdot \nabla)(\boldsymbol{\tau} + \mathbf{qn})] \qquad (12)$$

Assuming the fluid is incompressible, the Naiver-Stokes equations is given by:

$$\rho\left(\frac{\partial \mathbf{v}}{\partial t} + (\mathbf{v} \cdot \nabla)\mathbf{v}\right) = -\nabla p + \nabla \cdot \left(2\mu\mathbf{D}(\mathbf{v})\right) + \oint_\Gamma \mathbf{f}_\Gamma \delta^{(3)}(\mathbf{x} - \mathbf{x}_\Gamma)\mathrm{d}\Gamma \qquad (13)$$

This is the basic formulation of the immersed boundary method. ρ is the density, p is the pressure, μ is the dynamic viscosity, $\delta^{(3)}(\mathbf{x})$ is the three-dimensional delta function and $\mathbf{D}(\mathbf{v}) = (\nabla\mathbf{v} + \nabla\mathbf{v}^{\mathrm{T}})/2$ is the strain rate tensor.

In order to consider the different physical properties of the inner and outer regions, an indicator function is defined as,

$$I(\mathbf{x}) = \begin{cases} 1, \mathbf{x} \in \Omega_1, \\ 0, \mathbf{x} \in \Omega_2. \end{cases} \qquad (14)$$

Then the volume-of-fluid (VOF) function of a point $\mathbf{x}$ is defined as an integral over a small volume $\delta V(\mathbf{x})$,

$$\phi(\mathbf{x}) = \frac{\int_{\delta V(\mathbf{x})} H(x')\mathrm{d}V'}{\int_{\delta V(\mathbf{x})} \mathrm{d}V'} \qquad (15)$$

Therefore, the density and viscosity are written as following,

$$\begin{cases} \rho = \phi\rho_1 + (1-\phi)\rho_2, \\ \mu = \phi\mu_1 + (1-\phi)\mu_2. \end{cases} \qquad (16)$$

3. Result

In the present simulation, the normal elastic shear modulus is set $5.0 \times 10^{-6} N/m$, which is denoted by E_{s0}. We study seven cases with E_s/E_{s0} varying from 1 to 7, where E_s denotes the elastic shear modulus. The initial cell shape is a normal

biconcave shape with reduced volume of 0.64 in all the seven cases.

(1) Shape and deformation

Figure 1 shows the shape changes of RBCs with different E_s. Initially the RBC is put at the center of the tube with zero velocity. We are more concerned about the steady state of the RBC in narrow tube, so the large $10\mu m$ tube isn't long enough to get a full developed flow or the steady state of the RBC, which is the reason why the shapes of RBCs with different E_s in $10\,\mu m$ tube are nearly the same parachute shape. The RBCs exhibit different deformation while they are squeezing into the narrow tube (location Ⅱ in fig. 1). The RBC with large E_s take on more buckling, which means that a more stiff RBC needs more time to balance its shape and relax its local stresses. And we can see that they take on different shape at location Ⅲ after they enter the narrow tube. The rear of the more rigid RBC is convex compared with the concave tail of the softer RBC. After the RBC travels a long distance in the narrow tube(location Ⅳ in fig. 1), the RBCs with different E_s reach distinct final shapes. The relatively soft RBC has a more symmetric shape while the more rigid RBC exhibits an asymmetric shape with buckling on its side.

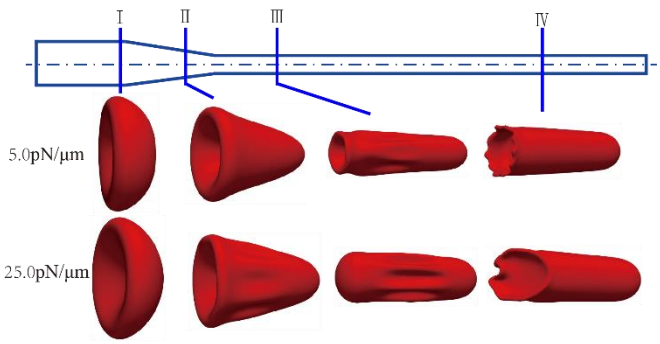

Fig.1. The shape evolution with time. The first line is a RBC with E_s of $5.0pN/\mu m$ The second line is a RBC with $25.0pN/\mu m$. Ⅰ, Ⅱ, Ⅲ, Ⅳ correspond to different location or different state of the cell motion. Ⅰ: the head of the cell reaches the end of the bigger tube where $x = 20\mu m$ ($x = 0$ corresponds to the inlet). Ⅱ: the head of the cell reaches the end of the end of the constriction tube where $x = 40\mu m$. Ⅲ: the rear of the cell arrives at the end of the constriction tube which means the cell totally squeezes into the narrow tube. Ⅳ: the cell reaches a steady shape.

To study the deformation of the RBC quantitatively, we define a deformation parameter L_c, which represents the length occupied by RBC at the central axis(shown in fig 2).It can partly represent the average length of the RBC. The result of a RBC with E_s of $10.0pN/\mu m$ is shown in fig 3. Figure 3 (a) shows the changes of L_c with time t(the RBC starts to move at $t = 0$). Figure 3 (b) shows the changes of L_c with x_c, where x_c is the location of the membrane centroid(x_c=0 at the inlet).

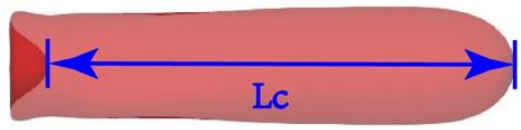

Fig.2. The definition of L_c. L_c is the length occupied by RBC at the central axis.

(a)

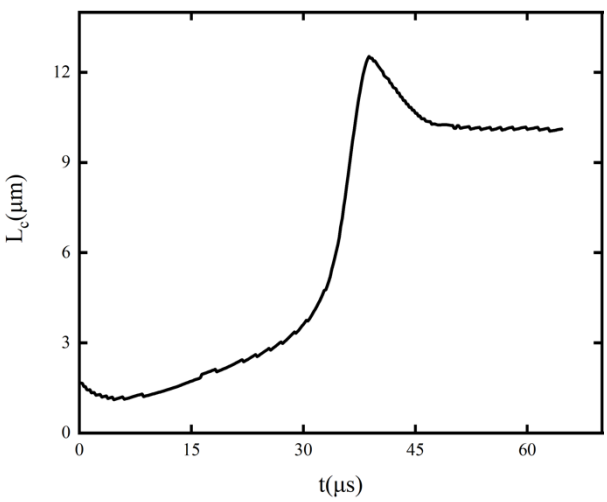

(b)

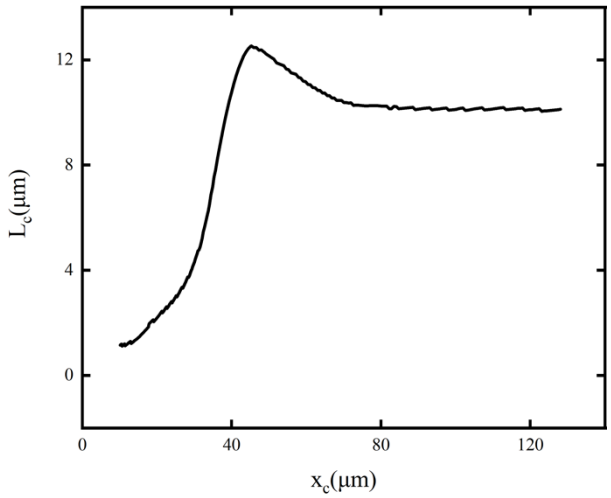

Fig.3. The change of L_c of a RBC with E_s of $10.0pN/\mu m$ while moving. L_c is the length occupied by RBC at the central axis. (a) The change of L_c with time t. (b) The change of L_c with x_c, where x_c is the location of the membrane centroid(x_c=0 at the inlet).

We can see from fig 3(b) that L_c decreases from the maximum value after the RBC entering the narrow tube. This means the RBC begin to relax after the large deformation in the constriction tube. Finally, L_c reaches a steady value. We study the maximum and steady value of L_c as a function of E_s(shown in fig 4). The steady value is calculated by averaging the value of L_c over a time period when it is s. We can see both value decreases with the increase of E_s. When the E_s/E_{s0} increases from 1 to 7, the maximum value of L_c decreases from 13.26μm to 11.72μm. Its relative decrease is about 11.6%. And the steady value of L_c decreases from 10.26μm to 9.59μm.Its relative decrease is about 6.5%.

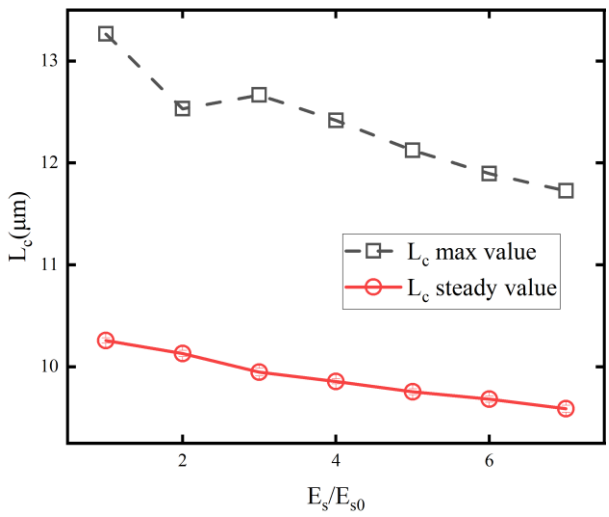

Fig.4. The steady and max value of L_c with different E_s. L_c is the length occupied by RBC at the central axis. E_s is elastic shear modulus. $E_{s0} = 5.0 \times 10^{-6} N/m = 5.0pN/\mu m$.

The high throughput microfluidic device measures the deformation or motion parameters to determine the mechanical parameters of the RBC. Figure 4 shows the steady value of L_c changes monotonically with E_s, which indicates that it can be used to measure E_s.

(2) Velocity

Figure 5 shows the velocity(denoted by v_c) change of a RBC with E_s of $10.0pN/\mu m$. Figure 5 (a) shows the changes of v_c with time t. Figure 5 (b) shows the changes of v_c with x_c.

(a)

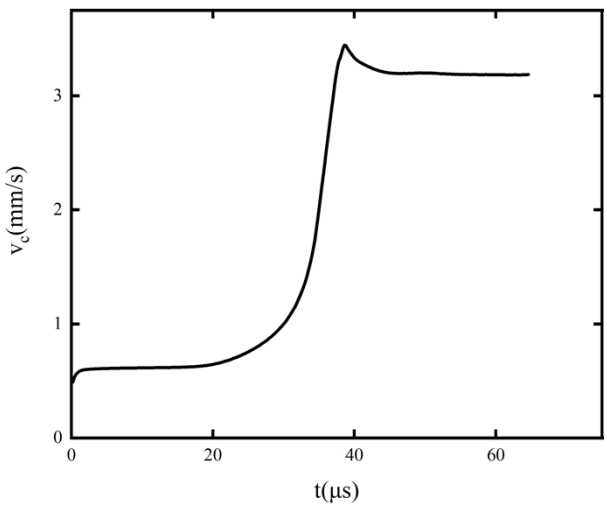

(b)

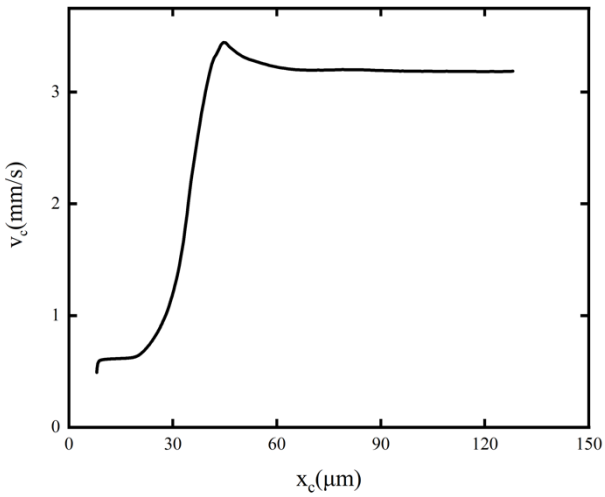

Fig.5. The velocity of the cell at different (a) time(t =

0 corresponds to the start time) (b) cell location (x_c is the location of the centroid of the cell).

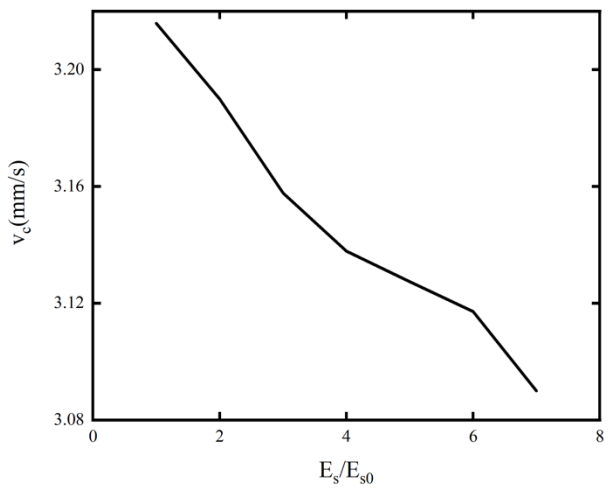

Fig.6. The steady velocity of the cell with different E_s. $E_{s0} = 5.0pN/\mu m$.

The value of v_c is relatively small when the cell starts. In the constriction tube, v_c increases rapidly and reaches peak. Then v_c decreases to a steady value in the narrow tube. Figure 6 shows the steady value of v_c with different E_s. This value is calculated by averaging the velocity over a period when the velocity is near constant. When the E_s/E_{s0} increases from 1 to 7, the steady value of v_c decreases from $3.216mm/s$ to $3.090mm/s$. Its relative decrease is about 4%. To explain this relation between v_c and E_s, the average lubrication layer thickness(denoted by $\bar{\delta}$) between the cell and the wall is calculated. The x axis is aligned with the flow direction. $\boldsymbol{n}$ denotes the membrane normal vector pointing outward. θ denotes the angle between $\boldsymbol{n}$ and x axis($\theta \in [0, \pi/2]$). $\mathbb{C}$ represents the set of membranes points on which $15° \leq \theta \leq 75°$ is satisfied. $\forall \mathbf{X} \in \mathbb{C}$, $\delta(\mathbf{X})$ represents the minimum distance between $\mathbf{X}$ and the tube wall. Then $\bar{\delta}$ is calculated as following:

$$\bar{\delta} = \frac{\int_{\mathbb{C}} \delta(\mathbf{X}) dS}{\int_{\mathbb{C}} dS} \qquad (17)$$

We calculate the average value of delta over a time period as the final result.

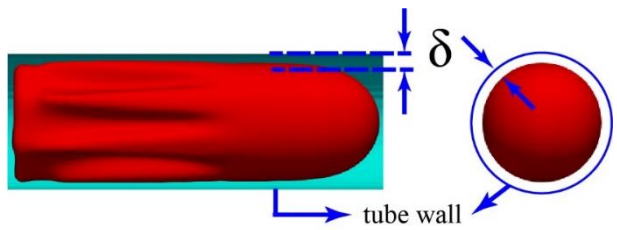

Fig.7. The definition of δ.

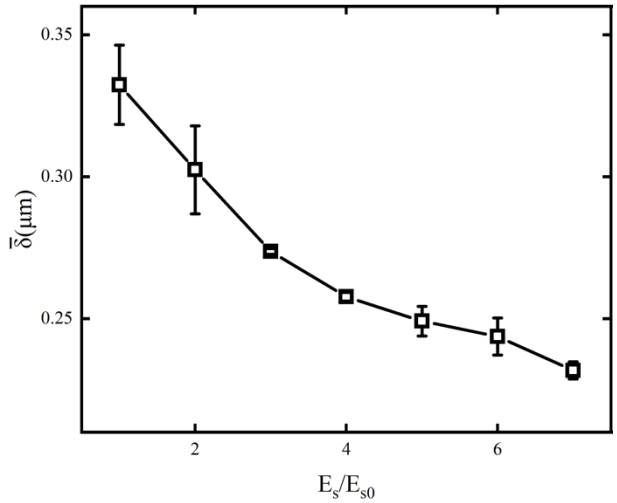

Fig.8. The average lubrication layer thickness with different elastic shear modulus. Some err bars are too small to see.

Figure 8 shows the value of $\bar{\delta}$ with different E_s. We can see $\bar{\delta}$ varying from 0.23~0.33 which is much less than the diameter of the narrow tube($d = 4\mu m$). $\bar{\delta}$ decreases monotonically with E_s increasing. This is due to the loss of deformation ability. Note that the diameter of the RBC is $7.82\mu m$ while the diameter of the narrow tube is $4\mu m$. The more rigid RBC will occupy more area of the cross section, which results in the decrease of $\bar{\delta}$. Then we relate $\bar{\delta}$ with the steady velocity of the RBC by lubrication theory..

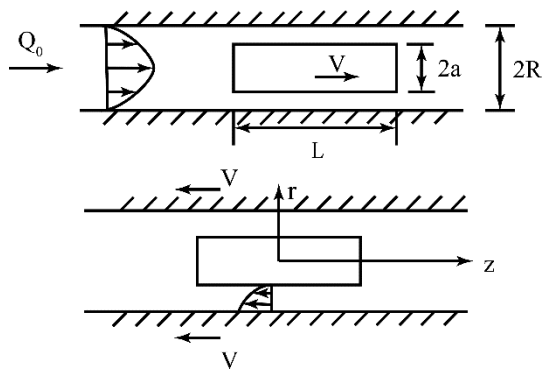

Fig.9. The physical model. A cylinder is moving at a

constant velocity V in a long circular cross- section tube toward right. The diameter of the cylinder is a, the tube is R. Take the cylinder as the reference frame then establish a cylindrical coordinate system.

Consider a cylinder moving at a constant velocity in a tube with infinite length. Homogeneous fluid fills the tube with a viscosity μ. The diameter and length of the cylinder is $2a$ and L, respectively. The diameter of the tube is $2R$. Q_0 is the flow rate. $h = R - a \ll R$.

Assume the velocity of the cylinder is V.Take the cylinder as the reference frame. Then the tube move at a velocity of V toward left. Establishing a cylindrical coordinate system as shown in fig.9. z axis is aligned with the flow direction. Velocity vector is denoted by (u_r, u_θ, u_z). Then we study the flow in the gap between the tube and the cylinder. Due to the symmetry in this case, we have $u_\theta = u_r = 0$. Then according to the incompressibility of the fluid, we can derive $\partial u_z/\partial z = 0$. Then list the momentum equation as following:

$$\frac{\partial p}{\partial r} = 0 \qquad (18)$$

$$\frac{\partial p}{\partial \theta} = 0 \qquad (19)$$

$$\frac{\partial p}{\partial z} = \frac{\mu}{r}\frac{\partial}{\partial r}\left(r\frac{\partial u_z}{\partial r}\right), \qquad (20)$$

Where p is the pressure.

The boundary condition:

$$\begin{cases} u_z|_{r=R-h} = 0, \\ u_z|_{r=R} = -V. \end{cases} \qquad (21)$$

Let $\partial p/\partial z = \xi$, we can get:

$$u = \frac{\xi^2}{4\mu}r^2 + c_1 \ln r + c_2 \qquad (22)$$

$$c_1 = \frac{\frac{\xi}{4\mu}(R^2 - (R-h)^2) + V}{\ln(R/(R-h))} \qquad (23)$$

$$c_2 = -\frac{\xi}{4\mu}(R-h)^2 - c_1 \ln(R-h) \qquad (24)$$

Considering the equilibrium of the cylinder in z direction:

$$\pi(R-h)^2 \times \left(-\frac{\partial p}{\partial z}L\right) = 2\pi(R-h)L \times \mu \frac{\partial u_z}{\partial r}\bigg|_{r=R-h} \qquad (25)$$

Considering the flow rate along the tube is constant, we have:

$$Q_0 = \pi R^2 V + \int_{R-h}^{R} 2\pi r u_z dr \qquad (26)$$

Finally, we can derive:

$$V = \frac{2Q_0}{\pi[R^2 + (R-h)^2]} \qquad (27)$$

$$\frac{\partial p}{\partial z} = \xi = -\frac{8Q_0\mu}{\pi(R^4 - (R-h)^4)} \qquad (28)$$

The average lubrication layer thickness $\bar{\delta}$ corresponds to h in equation(27), which shows the cylinder velocity decreases with h decreasing. Equation (28) shows that the absolute value of the pressure gradient increases with h decreasing, which indicate the pressure needed to keep the flow rate constant increases. So when the elastic shear modulus(E_s) increases, it will decrease the lubrication layer thickness which increase the flow resistance and finally slow the RBC. In next part, we study the flow resistance caused by the cell. As we can see, while the elastic shear modulus increases by six times, the steady value of the cell velocity decreases by 4%, which is relatively small.

(3) Extra pressure drop

The extra pressure drop is defined as following:

$$\Delta p_{extra} = \Delta p - \Delta p_{\text{Poiseuille}} \qquad (29)$$

Where Δp is the pressure needed to push the cell moving in the plasma and the $\Delta p_{\text{Poiseuille}}$ is the pressure needed to push the plasma moving at the same flow rate, just as shown is fig 10. Given the flow rate Q, the fluid viscosity μ and the diameter D of the tube, we can rewrite equation (29) as following:

$$\Delta p_{extra} = \Delta p - \frac{128\mu QL}{\pi D^4} \qquad (30)$$

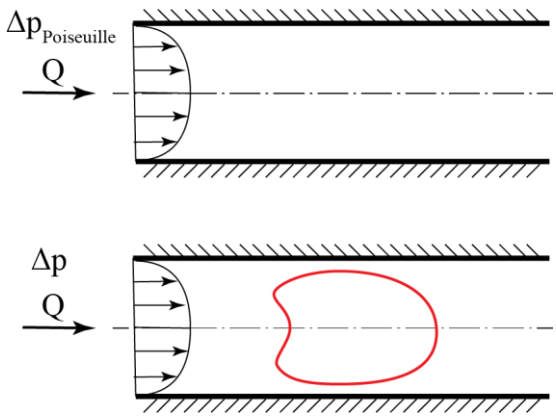

Fig.10. The first one is the Poiseuille flow without cell. Q is the flow rate, and $\Delta p_{\text{Poiseuille}}$ is the corresponding pressure. The second one has a cell in the tube with the same flow rate, but the pressure needed is higher than the first one, which means $\Delta p > \Delta p_{\text{Poiseuille}}$.

The extra pressure drop represents the increase of flow resistance due to the existence of the cell. In our simulation. The cell velocity is basically steady at $t = 50\mu s$. So we calculate the extra pressure drop with different E_s at $t = 50\mu s$. As fig.11 shows: extra pressure drop increases rapidly with cell hardening, which means the harder cell bring larger flow resistance. This result is also qualitatively consistent with the result of lubrication theory.

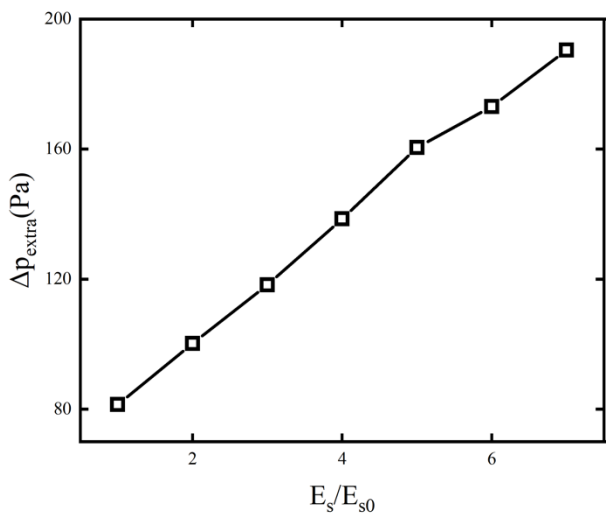

Fig.11. The extra pressure drop with different E_s.

As we can see, while the elastic shear modulus increases by six times, the extra pressure drop increases by 145%, which is considerably larger than the changes of the steady velocity (~4 %). In our previous modeling that treats the cell as a cylinder, the average lubrication layer thickness is a key parameter. The increase of elastic shear modulus results in the reduction of the layer thickness (shown in fig 8). Thus influence the extra pressure drop which represents the flow resistance caused by the cell. The simulation result shows that the extra pressure drop is more sensitive to the lubrication layer thickness than the velocity while the thickness is mainly determined by the elastic shear modulus. Therefore, the extra pressure drop is a sensitive parameter to elastic shear modulus change and can serve as an index to represent it.

4. Conclusion

We simulated the motion and deformation of a single red blood cell in a narrow circular-section tube with diameter of $4\mu m$. The influences of elastic shear modulus E_s are studied. Firstly, we study the shape evolution of the cell. We find that the final shape of the cell is usually an asymmetric shape. Then we find that in such a narrow geometry the influence of E_s on the cell velocity is little. This is partly due to the finite changes of the lubrication layer thickness. We find there is a monotonic relationship between the velocity with E_s. And we give an explanation for this using lubrication theory. The extra pressure drop which shows the flow resistance caused by the cell is also studied. We find this parameter is relatively sensitive to the changes of E_s.

5. Schedule and prospect for the future

In the future, we'll continue to numerically study the interaction of the secondary flow in a curved pipe with multiple cells to assist and direct the separation of rare blood cells such as circulating tumor cells (CTC) using a microfluidic device which mainly consists of a curved pipe. We will systematically study the behavior of multiple cells under different cell mechanical properties, volume fraction and flow boundary conditions to find the appropriate condition to achieve a good separation result. Our numerical

simulation is very important for the separation by using a curved pipe and design of corresponding experiment condition and microfluidic device. Therefore, we want to get the continuous support from RIKEN Supercomputer System in the FY 2020.

References:

[1] Noguchi H, Gompper G. Shape transitions of fluid vesicles and red blood cells in capillary flows[J]. Proceedings of the National Academy of Sciences, 2005, 102(40):14159-14164.

[2] Mebius R E, Kraal G. Structure and function of the spleen[J]. Nature Reviews Immunology, 2005, 5(8):606-616.

[3] Freund J B, Orescanin M M. Cellular flow in a small blood vessel[J]. Journal of Fluid Mechanics, 2011, 671:466-490.

[4] Park Y K, Diez-Silva M, Popescu G, et al. Refractive index maps and membrane dynamics of human red blood cells parasitized by Plasmodium falciparum[J]. Proceedings of the National Academy of Sciences, 2008, 105(37):13730-13735.

[5] Skalak R, Tozeren A, Zarda R P, et al. Strain Energy Function of Red Blood Cell Membranes[J]. Biophysical Journal, 1973, 13(3):245-264.

[6] Pozrikidis C. Effect of membrane bending stiffness on the deformation of capsules in simple shear flow[J]. Journal of Fluid Mechanics, 2001, 440:269---291291.